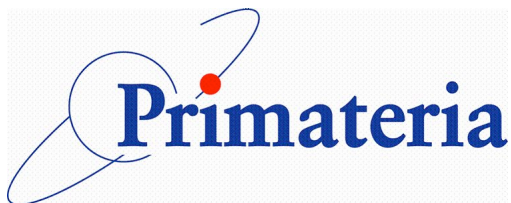


Peter Stuesson
Examensarbete 30 hp
Teknisk Fysik med Materialvetenskap
Uppsala Universitet
Primateria AB

Friction characteristics between ski base and ice -fundamental lab scale tests and practical implications



Abstract

The friction between skis and snow is governed by a very complicated set of parameters. One of the biggest difficulties in analysing the situation – and thereby being able to optimise the skis for low friction gliding – lies in the variability of the snow. The properties of the snow are highly dependent on temperature, density, resulting hardness, relative humidity etc. Other variables that are hard to keep constant include the skier, the wind, the condition of the ski wax, etc. For this thesis, ice is used to represent an extreme case of snow.

In order to increase the understanding of some of the governing phenomena, while keeping the unintended variations as low as possible, a simplified test rig has been built and a set of experiments has been conducted. The test rig comprises a small rotating snow/ice-covered disc and a small model ski, all included in a chest freezer. The load and speed was chosen to represent cross-country skiing and the temperature was varied to represent different skiing conditions, from cold and dry to above zero and wet.

The model ski was given different kinds of surface preparations and the sliding friction was monitored against varying load, velocity, and air and ice temperature.

The resulting friction is reported and correlations with snow friction and the practical implications for optimum ski preparation for different conditions are discussed.

Sammanfattning

Hur en skida glider på snö är ett fenomen som sedan länge engagerat allt från den enskilde åkaren till forskning och industri. Glidmotståndet, friktionen, mellan skida och snö är en systemparameter med ett komplext beroende av ett antal andra parametrar.

För att två ytor överhuvudtaget ska kunna glida mot varandra krävs en deformation i den mikroskopiska kontakten. Denna kontakt utgörs av ett antal punkter om ungefär 0,1 mm diameter, summerade ger dessa den reella kontaktarean som är i storleksordningen promille av den nominella, dvs. skidans yttre dimensioner över glidområdena. Deformationen vid glidning är antingen av torr eller våt karaktär. Torr karaktär ger att adhesiv skjuvning eller plogning av ytornas ojämnheter bestämmer motståndet. Konservativt sett så att det mjukaste materialet är det som deformeras lättast och därmed bestämmer både plogmotståndet och den reella kontaktytan. Våt karaktär innebär för de typiska temperaturerna och hastigheterna att en separerande vattenfilm skjuvas laminärt på grund av ytadhesion och ojämnheter i belaget. Detta motstånd karaktäriseras av vattenfilmens viskositet, filmtjocklek och kontaktarea. Vid en hastig minskning av filmtjocklek och utbredning av kontaktytan kan glidmotståndet öka drastiskt vilket brukar upplevas som att skidorna sugts fast i snön. En teoretisk formulering och materialbeskrivning visar att variationer i hastighet, last och temperatur är lämpliga för att karaktärisera glidmotståndets natur.

Den mest komplexa parametern är snön och dess variabilitet. Snö är ingen solid fas av vatten utan en matris av korn, i sig uppbyggda av is. Detta innebär att snöns mekaniska egenskaper dels beror på hur enskilda korn i mikroskopisk skala beter sig och dels hur dessa gemensamt och relativt beter sig i den makroskopiska skalan. Snöns densitet styr både elasticitetsmodulen och den makroskopiska hårdheten och är kanske den viktigaste indikatorn på glidförutsättningarna vid en viss tidpunkt. Vid maximal densitet, elasticitetsmodul och hårdhet är snö och is ekvivalenta. Snöns yta är mycket porös och ojämn, även i ett välpreparerat spår, därtill gör skidbelagets grova yta att den topografiska interaktionen mellan ytorna kan antas ha stor inverkan på en skidas förmåga att glida.

Som ett första steg mot att simulera skidåkning och öka förståelsen för friktionens karaktär har en enkel testutrustning konstruerats och ett antal verifierande experiment har genomförts. Utrustningen består av en rigg med en 500 mm roterande istäckt skiva och en miniatyrskida av ett typiskt belagsmaterial med konventionell ytkaraktäristik. Skidan hålls i en fritt lagrad arm och fixeras av en trycksensor. Allt glidmotstånd tas upp i trycksensor varvid friktionen kan noggrant mätas. Hela utrustningen är placerad i en frys. En isyta är använd

Inledande tester visar att glidmotståndet domineras av en torr karaktär för temperaturer under -10°C . En övergående fas mot våt karaktär sker ju närmare man kommer 0°C . Ur ett tribologiskt perspektiv implicerar detta att skidbelaget alltid ska vara så slätt som möjligt i åkriktningen, där reell kontakt uppstår. Vid ökande våta förhållanden ska en struktur läggas in i belaget för att förhindra att vattenkontakten breder ut sig och om nödvändigt dränera ytgränssnittet, likt bildäck som ska förhindra vattenplaning.

1. INTRODUCTION	5
1.1 PROBLEM AND BACKGROUND	6
1.2 PURPOSE OF THE PROJECT	6
1.3 LIMITATIONS	6
2. THEORY	8
2.1 DRY FRICTION – ADHESION AND PLOUGHING	8
2.2 WET FRICTION	10
2.3 FRICTION HEAT	11
3. INTERACTING MATERIALS – ICE/SNOW/WATER AND SKI BASE.....	13
3.1 PHYSICAL AND MECHANICAL PROPERTIES OF ICE AND SNOW	13
3.1.1 <i>Solid phase structure – ice and snow</i>	13
3.1.2 <i>Microscopic hardness - ice</i>	14
3.1.3 <i>Macroscopic hardness - snow</i>	14
3.1.4 <i>Hardness correlation between ice and snow</i>	15
3.1.5 <i>Surface properties</i>	15
3.1.6 <i>Lubricating water layer</i>	16
3.2 PHYSICAL AND MECHANICAL PROPERTIES OF THE SKI BASE	17
3.2.1 <i>Solid phase structure</i>	17
3.2.2 <i>Microscopic hardness</i>	17
3.2.3 <i>Surface properties</i>	19
3.2.4 <i>Real contact area establishment</i>	22
3.3 WEAR	22
4. EXPERIMENTAL APPARATUS	24
4.1 CONSTRUCTION OF CUSTOM MADE TRIBOMETER	24
4.1.1 <i>Basic</i>	24
4.1.2 <i>Experimental setup</i>	25
4.1.3 <i>Motor system</i>	25
4.1.4 <i>Analytical equipment</i>	26
<i>System parameters</i>	27
<i>Value</i>	27
4.2 EXPERIMENTAL	28
4.2.1 <i>Test samples</i>	29
4.2.2 <i>Track preparation</i>	30
5. RESULTS	31
5.1 TEST APPARATUS	31
5.2 VELOCITY DEPENDENCE	31
5.3 LOAD DEPENDENCE	33
5.3.1 <i>Surface comparison</i>	34
5.4 TEMPERATURE DEPENDENCE	35
6. DISCUSSION	36
6.1 TEST APPARATUS	36
6.2 VELOCITY DEPENDENCE	36
6.3 LOAD DEPENDENCE	37
6.4 TEMPERATURE DEPENDENCE	37
6.5 SURFACE PREPARATION	38
7. CONCLUSIONS	39
7.1 TRIBOMETER	39
7.2 FRICTION BEHAVIOUR	39
7.3 SURFACE PREPARATIONS	39
REFERENCES.....	40
WEB SOURCES.....	42

1. Introduction

Skiing has a certain place in the cultures of Scandinavia, from the use of transport through snow-covered landscapes to a huge sport with a surrounding commercial business. Increasingly hindered by a warmer climate, skiing still seems to be highly regarded as an elite sport as well as recreation. Since much of the experience with skiing is based on the gliding phenomenon there is a huge interest and strife towards improving the gliding ability. This work has been in progress at least since the 1930's and has been seriously undertaken various times since. An important step for ski friction research would be overlapping the gap between theoretical descriptions and experimental results and further on with field tests and ski preparation methods. Since the subject is so closely connected with the specific practice of skiing it is certainly in the interest of all to reach conclusions of how to increase the gliding ability of skis.

Research has been made on the tribosystem of ski base against snow and/or ice through the years. Add to this all the material specific work that has been made upon ski base materials, ice and snow. A short summary of relevant work from the past and present is given below:

- [1953] Bowden, a pioneer within tribology, describes various friction phenomena for skis out of perspective of material hardness, contact area, friction heat and hydrophobicity.
- [1968] Fletcher publishes theoretical calculations describing the presence of a liquid-like amorphous surface layer on ice.
- [1974] Katutosi develops a method to measure the macroscopic hardness of snow showing temperature dependence within specific snow types and a much softer nature than that of solid ice.
- [1974] Gow describes the time-temperature sintering of snow, concluding that it behaves similar to any other powder compact, at a very slow pace though.
- [1978] Golecki and Jaccard measure the intrinsic surface disorder of ice with results correlating to Fletchers calculations. They measure a temperature-dependent quasi-liquid surface layer as thick as 100nm near the melting point.
- [1984] Spring measures ski friction as a function of temperature and states a number of parameters, frictional as well as aerodynamical, affecting the glide. The experiments consisted of field tests with a skier running down a specific slope.
- [1988] Colbeck describes a number of friction mechanisms, assuming a shearing of water and electrical charging as relevant parameters.

- [1989] Lehtovaara presents a theoretical friction model concerning dry, lubricated and mixed mechanisms. He concludes a dependence of friction on temperature, load, velocity and number of contact spots.
- [1999] Moldestad shows the behaviour and importance of water content in the snow.
- [2005] Kuzmin rejects the idea of ski wax for glide preparation due to an unnecessary dirt adhesion. He further concludes that a steel scraper can prepare the ski base in a better way.
- [2006] Baurle refines many of the measuring principles performed by Lehtovaara and concludes a similar friction model.

1.1 Problem and background

During early studies it was found that there are numerous of diverging theories about the gliding abilities of skis. As a feasibility study into the realms of ski preparation, conventionally prepared ski base surfaces were studied with light optical profilometry and scanning electron microscopy. These surfaces were believed to be far from optimal and further studies were required. Some of these will be shown in this thesis.

The Ångström laboratory of Uppsala University and Primateria AB joined forces in the project. This fusion provided resources of laboratory equipment and the vast knowledge concerning surface preparation. It was also considered that valuable results should be embodied in a product suitable for an everyday skier to use.

1.2 Purpose of the project

A basic tribological ski friction-theory will be used in order to reveal and later on evaluate possible and important friction mechanisms. In order to isolate and verify these mechanisms a custom made test apparatus will be designed and built. It is an aim to characterize general friction behaviour and later on attain such measurement resolution that different surface preparations can be relatively compared and evaluated. Correlations between results and previous literature as well over bridging the gap onto ski preparation according to theory and results will be discussed.

1.3 Limitations

The tribosystems in focus is ski base-snow with ski base-ice as an extreme. Therefore, parameters such as apparent contact area, ski span, nominal pressure distribution, ski length and width are not considered in the theory and experiments. These parameters affect the prerequisites for different mechanisms but are not actual friction mechanisms.

Areas where low friction is essential are studied. These are the glide areas of a classic ski and the whole of a skate ski, alpine ski and snowboard. This excludes the kick area and the grip/kick wax issue.

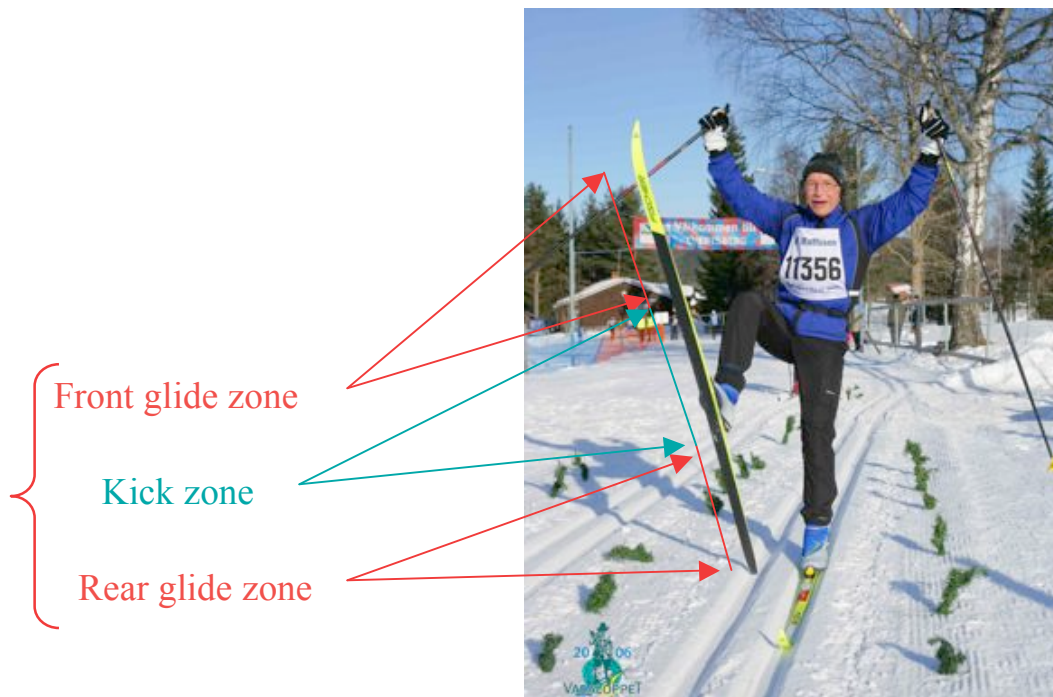


Figure 1: Expose of the typical friction zones of a classic ski performed by Professor Sture Hogmark at the Vasaloppet race 2007.

Emphasises in the project is put upon the ski base topography as the primary parameter for reducing friction. No wax or other additive, assumed to decrease friction, is used in the experiment.

The initial experiment series is very limited due to the twenty-week time restriction for the thesis work.

2. Theory

The dynamic system of two surfaces in relative motion is a tribological system and is conveniently described by following theory. Parameters used in this section are listed and defined below:

- a_i – Arbitrary area of a contact spot
- A_r – Total dry real contact/load carrying area
- A_p – Contact area projected in the motion direction
- A_w – Total wet contact/load carrying area
- f_i – Arbitrary normal force exerted on a single contact spot
- F_N – Total normal load i.e. the weight of a skier
- F_T – Total friction force
- H – Hardness
- τ_y - Maximum shear stress of a solid material
- μ - Friction coefficient, adhesive, ploughing or wet
- Re – Reynolds number
- v – velocity
- h – lubricating water film thickness
- η - Dynamic viscosity
- S – Velocity gradient
- T – Temperature
- t – Contact time
- σ_0 – Maximum nominal pressure
- D – Diameter of single contact spot
- P – Effect
- q – Heat flux
- ρ - Density
- λ - Thermal conductivity
- c_p – Specific heat capacity

SI-units or units derived from SI-units are used for all parameters.

2.1 Dry friction – adhesion and ploughing

When two surfaces, assumed to have a roughness above ideal smoothness, are pressed together they collide at many microscopic contact spots with individual areas a_i . Summarized they will constitute the real contact area A_r :

$$A_r = \sum_{i=1}^n a_i \quad (1)$$

Note that this sum will be much smaller than the nominal, visually expected, area. These small areas will carry the load f_i placed upon them, thus the sum of forces will constitute the normal load F_N :

$$F_N = \sum_{i=1}^n f_i \quad (2)$$

With an applied load the contact spots will increase in area or in numbers in order to be able to carry the load. The load will together with the hardness H of a material and the size of a contact spot determine f_i and a_i :

$$a_i = \frac{f_i}{H} \quad (3)$$

Out of two different materials the softer will yield before the harder, thus determining A_r . If all previous formulas are combined the contact area can be expressed as:

$$A_r = \sum_{i=1}^n a_i = \sum_{i=1}^n \frac{f_i}{H} = \frac{F_N}{H} \quad (4)$$

If the surfaces begin a relative motion aligned with the contact plane the contact areas will move and deform. The deformation resistance will consist of the shear stress of every contact spot of the softer material, thus the friction force will be:

$$F_T = \sum_{i=1}^n a_i \tau_y = A_r \tau_y \quad (5)$$

The friction coefficient is a quota between friction and normal force:

$$\mu_a = \frac{F_T}{F_N} = \frac{A_r \tau_y}{A_r H} = \frac{\tau_y}{H} \quad (6)$$

Considering that the pressure on a surface activates a larger volume of the bulk material, the friction coefficient for a system with a thin dry lubricating coating can be expressed as a quota between the shear stress of the coating and the hardness of the bulk material [Jac05]:

$$\mu_a = \frac{\tau_y}{H} \left(1 + \beta \frac{\tau_y}{H} \right)^{\frac{1}{2}} \quad (7)$$

where β is a material constant. The important issue is the governing of the smallest shearing resistance determining the shear stress while the softest material determines the contact area.

On a rough surface, asperities will collide mechanically in large numbers and for a constant load the friction will consist of the projected collision areas and the resistance against deformation $\approx H$:

$$F_p = A_p H \quad (8)$$

But with a varying load both the normal load carrying force and the friction force will depend on the hardness together with load carrying and ploughing areas A_r and A_p respectively:

$$\mu_p = \frac{A_p H}{A_r H} = \frac{A_p}{A_r} \quad (9)$$

If adhesive and ploughing friction mechanisms are independent from each other the dry friction force will in its entirety be described as:

$$F_T = F_N (\mu_a + \mu_p) \quad (10)$$

2.2 Wet friction

If a thin lubricating film separates the two surfaces, the topography will not have the same direct impact on friction. Shearing of the film will constitute the relative motion resistance. Consider a very thin film and no-slip condition between lubricant and surfaces. Water will at these orders of magnitude behave differently from those of water drops or running water. Motion of water is determined through its inertial momentum that describes the turbulent behaviour and the viscous momentum that describes the laminar behaviour, i.e. the Reynolds number shows the ratio between these two:

$$\text{Re} = \frac{vh}{\eta} \quad (11)$$

where v is velocity, h water film thickness and η the dynamic viscosity. For $\text{Re} \ll 1$ laminar flow can be expected and $\text{Re} \gg 1$ turbulent flow can be expected. [Pav07]

Using typical values for a Nordic skier, $v=5\text{m/s}$, $\eta=10^{-3}$, and $h=10^{-6}$, the Reynolds number will be 0.005. This is well below 1, indicating laminar flow. Even at downhill velocities, $v=30\text{m/s}$, $\text{Re}=0.03$. Together with the no-slip condition a velocity gradient for the water molecule layers can be simply described as:

$$S = \frac{v}{h} \quad (12)$$

where v is the velocity and h the thickness of the film. For a Newtonian liquid the viscosity is independent from load and thus the shear resistance will depend on the velocity gradient together with the viscosity:

$$\tau_v = \eta S \quad (13)$$

This shearing motion resembles the one for adhesive dry friction where the real contact area is constituted by the film area rather than the sum of contact spots. The combination of (5), (11) and (12) describes the viscous friction force as:

$$F_T = \tau_v A_w = \eta S A = \frac{\eta v_0 A_w}{h} \quad (14)$$

[Jac05]

The viscosity is temperature dependent and increasing for a decreasing temperature:

$$\eta = 2.414 \cdot 10^{-5} \cdot 10^{\frac{247.8}{T-140}} \quad (15)$$

Typical values for the viscosity of water at 0°C, 5°C and 10°C are $1.76 \cdot 10^{-3}$, $1.5 \cdot 10^{-3}$ and $1.3 \cdot 10^{-3}$ Pa*s respectively.

The water film can only be assumed to carry load for a time and a squeeze out-effect will occur. This can be described by the change in water film thickness:

$$\Delta h = \frac{16t\sigma_0}{3\eta D^2} \quad (16)$$

where D is the length of a contact, t is contact time and σ_0 the maximum pressure. For an assumed contact spot of 100µm diameter, velocity of 1 m/s, the load time of a spot is 10^{-4} s. The resulting thickness change is then from a 100nm thick film to 80nm. [Bäu06]

2.3 Friction heat

During dry contact, the heat momentarily produced in the ski-snow interface is:

$$P_{dry} = v\mu F_N \quad (17)$$

where v is the velocity, F_N the weight of the skier and μ the friction coefficient. The heat flux into the surfaces is then expressed as:

$$q = v\sigma_0\mu \quad (18)$$

where σ_0 is the maximum pressure on ice – the hardness H.

When a water film is present, further heat production is described by:

$$P_{wet} = \frac{\eta v^2}{h} \quad (19)$$

The amount of heat flowing into the different surfaces is governed by the thermal conductivity of the respective materials [Kur77]. The temperature change of any material can further be described as:

$$\Delta T = 2q \left(\frac{t}{\pi \rho \lambda c_p} \right)^{\frac{1}{2}} \quad (20)$$

where ρ is the density, λ the thermal conductivity and c_p the specific heat capacity.

There are more mechanisms suggested over the years, such as capillary drag and influence from electrostatic fields. These are not considered in the models and are not believed to be largely affecting parameters. Impact from capillary forces would demand a phenomenon where a surface tension of the water film is broken.

It is clear from the orders of magnitude of velocity and water film thickness, even for downhill racing and extremely thick films, that the fluid motion has a laminar character and therefore will be sheared. The strength of the adhesion forces between solid and liquid is not entirely relevant since any surface roughness would mechanically move the closest molecule layers causing a shearing anyway. Only for, on an atomic level, perfectly smooth surfaces with an ideal chemically hydrophobic preparation would the surface slip on the water film. The commonly observed phenomena of “suction” during conditions with high moisture and/or large presence of water, is easily explained by the extreme increase of contact area and decrease of water film thickness in eq (14).

Topographical impacts on hydrophobicity are somewhat confusingly presented in the scientific literature. Sometimes certain structures are created on a surface in order to increase the hydrophobicity, usually called ultra hydrophobic surfaces. This does not necessarily mean that water moves easier against a rough surface or that increased roughness is favourable. On the contrary, if the roughness causes a surface to break through the lubricating water film a dry ploughing will dominate the friction.

Structurized surfaces considered to be ultra hydrophobic are effective in their particular experimental system, usually with millimetre-sized water droplets, but will not necessarily be effective in other systems where for instance condensation can occur in the structure or where the water is of a different order of magnitude [Wie06]. Literature strongly supports that a smoother surface increases the hydrophobicity, especially during conditions where condensation is present. If hydrophobicity would matter in a large scale, surface refinement would still be for the better. [Tor03], [Wie06]

3. Interacting materials – Ice/Snow/Water and ski base

Water is obviously a very essential matter for this thesis. Presumably it will act both as a solid state material in the snow surface and as a liquid lubricator in the surface interface. The common properties of water such as density, molecular weight, melting point et cetera are well known. For the ski base-snow interface relevant material properties as important system parameters are discussed here.

All hardness magnitudes are here given in MPa and are recalculations from the Brinell scale.

3.1 Physical and mechanical properties of ice and snow

Snow is nothing but grains of ice with various and, possibly, individually unique geometry. Still a close-up view would show nothing but ice. As a macroscopically behaving material snow is nothing like solid ice but given the right prerequisites it might act with similar properties.

3.1.1 Solid phase structure – ice and snow

There are several possible phases of ice, all with different order and properties. Fortunately there is only one of them, 1h that exists in nature. This also includes artificial snow [Lib05]

The unit cell is hexagonal with a deviation of 0.3 degrees from an ideal one. The facets of the cell are responsible for the growth of an ice crystal. It can easily be observed that snow grains are six-folded, either dendritic or with facets.

Since 1h phase with a hexagonal structure is the only one to consider, it can be concluded that different shaped grains are based on the same material in terms of hardness and wear at a certain temperature. [Lib05]

Growth and geometry of the grains is controlled by pressure, humidity and temperature. It is necessary to observe two crystallization environments; the primary is in the air and the secondary on the ground. Grains are created in the air where the initial shape occurs. Recrystallization on the ground caused by varying temperature, or possibly by friction heat and pressure in a ski track, is a very significant parameter when the grains converges slowly towards a spherical shape. [Lib05]

An important parameter is the sintering that occurs over time [Gow74]. This implicates that grains grow in size and together over time to polycrystalline grains rather than single crystals.

3.1.2 Microscopic hardness - ice

A 1h ice single crystal has a temperature-dependent hardness described by Butkovich already in 1958. This shows a weak exponential relation with a typical hardness of 50 MPa at -10°C , see figure [But58]. For polycrystalline ice, the hardness is 5-25 MPa in the temperature interval -10°C to -20°C [Pet02]. Pittenger et al. have measured a hardness of 23 MPa at -10°C for polycrystalline 1h ice during this load time [Pit98].

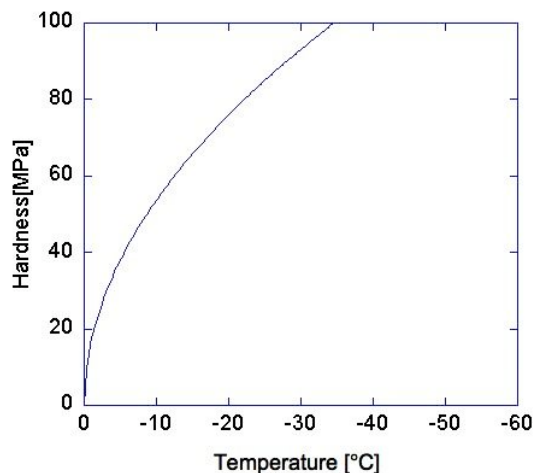


Figure 2: Single crystalline ice hardness vs. temperature. After [But58].

Ice has a visco-elastic component that implicates a load time-dependent hardness. Kuroiwa and Bäurle has shown that contact spot sizes between the ski base and the snow grains have, at typical load magnitudes, an average radius of 100-200 μm , maximum 400 μm , approximating a circular section [Kur77], [Bäu06]. For a skier at 1 m/s this represents a load time of 10^{-4} s on each grain.

Due to the sinter process of snow it can be assumed that large snow grains are polycrystalline clusters. The hardness of ice is therefore of varying magnitude and can be expected to be both harder and softer than the ski base. See section 3.2.

3.1.3 Macroscopic hardness - snow

In the Macroscopical perspective, snow will be packed when a load is placed upon it, thus acting as a different material than solid ice. This implicates that the elasticity module will be a system parameter for the hardness measurement. Katutosi has developed a method for hardness measuring of snow during a shock load of very short time, showing linear temperature dependence for a certain snow-type as well as a different order of magnitude. A typical value for large grained snow at -10°C is 500 kPa. It is notable that the elasticity modulus is governing the hardness. The density, perhaps being the most essential parameter for snow hardness, further determines the magnitude of these two. Temperature is therefore not the only affecting parameter for ice and snow hardness. [Kat74]

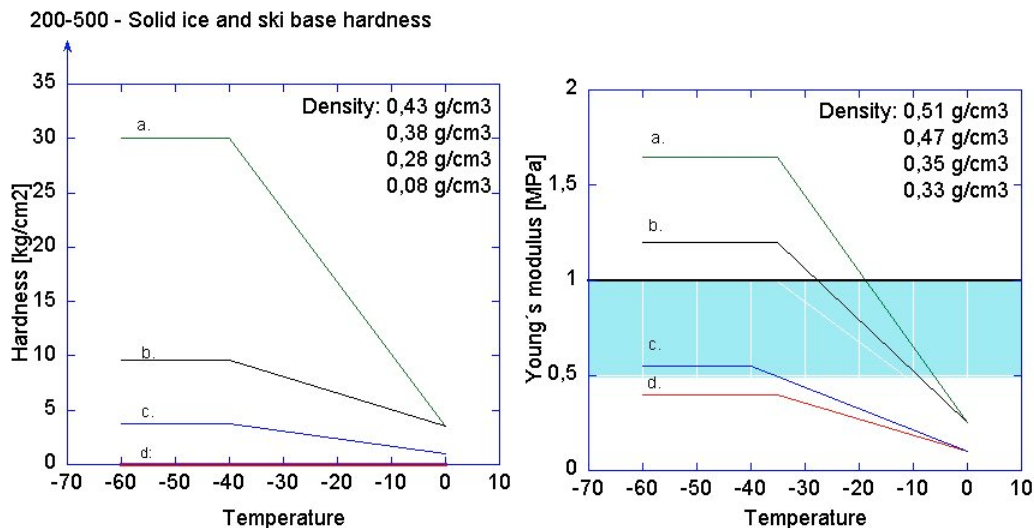


Figure 3: Hardness and elasticity modulus for different types of snow. a: artificially compacted snow, b: coarse-grained snow, c: fine-grained snow d: new snow. Note the increasing density along with the hardness. The blue-shaded area represents typical elasticity modulus of ski base materials. After [Kat74]

3.1.4 Hardness correlation between ice and snow

A comparison shows that for a skier of 80 kg, ice needs a static contact area of 35 mm² while the snow type b. needs 1600mm². This macroscopic area is still a surface consisting of snow grains. Assuming a grain diameter of 1mm, 2038 grains then constitutes the macroscopic area, equally many contact spots carries the load. Using the contact spot size measurements earlier mentioned, it can be shown that the area sum is somewhere between 30-60 mm², same order of magnitude as for solid ice. This indicates well that the correlation between the hardness of snow and ice is determined by the compaction of snow. This compaction is due to the extremely low elasticity modulus of snow, far smaller than for UHMWPE, which is about 0.5-1Gpa [Gur08]. The snow compaction is thus a density increasement towards a sufficient total hardness large enough to carry the load. The upper limit is of course the elasticity and hardness of solid ice.

If the temperature is close to 0°C, it can be imagined that the compaction of snow never reaches a steady state for each kick or skate of a skier. This would indeed result in a very large load carrying contact area of several cm². If so an expected friction increase would not only result in a widening of a large wet continuous contact area.

3.1.5 Surface properties

It has been suggested already in the 19th century, that a liquid-like layer covers the surface of ice. Studies during the 60:ies and 70:ies revealed that the surface of ice has characteristics of something in between solid and liquid. Different methods were used to determine the thickness of this layer. In 1978 Golecki and Jaccard examined the crystal order as a function of temperature at normal atmospheric pressure. A crystalline disorder was discovered, growing rapidly above -40°C, towards the crystal

core. With the amorphous structure growing inwards, the surface disorder also increased. Towards the melting point the amorphous layer took form of a quasi-liquid layer with a temperature dependent thickness described by $(94 \pm 17) - (54 \pm 14) \log(273-T)$ nm. At -20°C the thickness is slightly above 20 nm, at -10°C it is 40nm and close to 100 nm at 0°C . This is not necessarily to be taken for a liquid layer but rather a general thin soft surface layer. [Gol78] See figure 3:

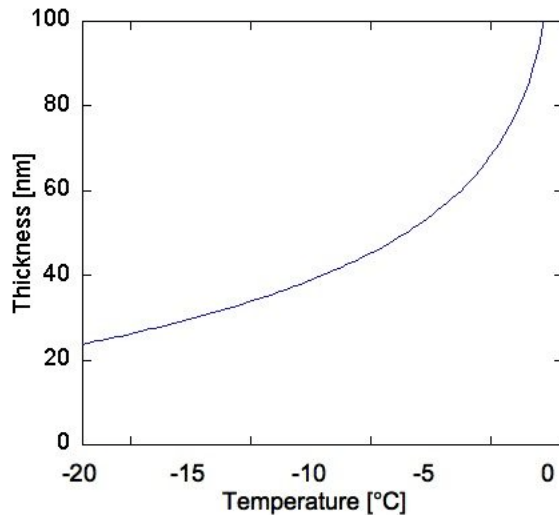


Figure 4: The root mean square of the growth of the amorphous surface layer.

3.1.6 Lubricating water layer

It is suggested that friction induced heat melts ice crystal asperities into a lubricating water film [Bow53], [Kur77], [Leh89], [Bäu06]. The water content can also be contributed through water presence in the snow at temperatures close to 0°C and through high relative air humidity [Mol99]. As already seen, a further contribution would be from the ever-present amorphous surface layer.

For friction heat, it can be assumed that the water film occurs where relative contact exists, this would implicate that lubrication initially occurs where dry friction produces the friction heat. Considering the behaviour of the growth of the amorphous layer, further heat would initially speed up the growth process resulting in a fully liquid surface layer.

Different attempts have been made to measure and estimate the thickness of the film since it is of vital importance for the understanding of viscous friction contribution. Ambach and Mayr show an in situ test where a probe is built into a ski. Their results shows a thickness of in the range of $5\text{-}13\mu\text{m}$ [Amb81]

Strausky et al. show in a more recent experiment that for low velocities, 0.1 m/s , at -2°C no film thicknesses above 50 nm and 250 nm respectively was present for a ski base of PMMA and ultra high molecular weight polyethylene, respectively. Evidently no film in the μm scale was needed for a friction coefficient of 0.03 in their system [Str98]. Theory shows that for increased velocity, proportionally more heat is

produced and for velocities of 1 – 10 m/s magnitudes of 100 nm to 1µm can be assumed out of Strausky's measurements. Baurle calculated film thicknesses out of his friction and contact area measurements showing thicknesses ranging from 100 nm to about 1µm.

If a spherical shape of a grain is assumed, a conservative calculation out of eq (17) shows that for a velocity increase from 0.1 to 10 m/s generates 100 times more heat thus melting a proportional larger volume of the grain. From the measurements of Strausky et al. the resulting order of magnitude for the melted layer is within 500 nm. It is therefore assumed that the lower orders of magnitude suggested by Baurle and Strausky are more reliable than those of Ambach and Mayr.

3.2 Physical and mechanical properties of the ski base

In the early days a thin hard wooden ski sole would be used as the base, prepared with tar over the open fire, finished off with paraffin, usually from a candle.

Today the ski sole or base is made of ultra high molecular weight polyethylene - UHMWPE, a polymer commonly used in artificial joints in body implants where low friction and high wear resistance are demanded.

3.2.1 Solid phase structure

UHMWPE is a polymer consisting of extremely long molecule chains consisting of between 500 000 and 10 500 000 monomers. The length of the molecule chains decreases the ability to align thus the crystallinity is about 40-50% and slightly decreasing with increasing molecule weight. This also affects the density and hardness and a mere 25g mass difference between lightest and heaviest ski soles. The intermolecular space in the amorphous regions is often filled with carbon particles. [Gur08].

Gurit AG manufactures most UHMWPE for ski bases under commercial names such as P-TEX. It is produced through extrusion except for the bases with longest molecule chains, being press-sintered.

3.2.2 Microscopic hardness

As mentioned the hardness is dependent on molecule weight. Being a polymer, UHMWPE is a visco-elastic material thus having a time-dependent hardness [Suw98].

The time-dependence implies that the hardness increases severely if the load-time is very short. Development over time has led to severely increased hardness of UHMWPE [Bow53], [Liu99]. Today the hardness of UHMWPE is between 30 and 90 MPa already at room temperature and can be expected to increase at lower temperatures.

The hardness and wear resistance is typically increased by adding particle fillers to the UHMWPE matrix [Suw98], [Liu99], [Gur08]. The time-dependence is still

unaffected [Suw98]. Further reinforcements with carbon fibres increase both hardness and wear resistance [Dan04]. See figure 4:

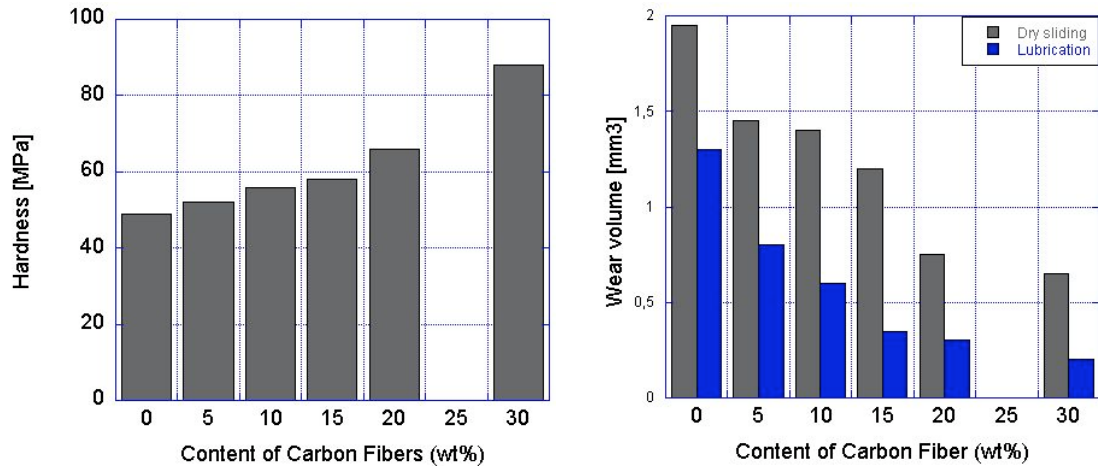


Figure 5: Hardness and wear resistance respectively of UHMWPE vs. carbon fibre reinforcement. Wear test made against steel. Diagram after [Dan04]

3.2.3 Surface properties

Compared to metals and ceramics, UHMWPE is a very soft material and tool preparation of the surfaces is assumed to show material behaviour that differs from these. All following topographical figures are presented in the same height and colour scale. Green represents the mean value and red and blue top and bottom respectively.

The basic preparation of a commercially bought Nordic ski is stone grinding. This is considered as a reference surface since most people ski on the structure given by this preparation, even if additional preparations bring some differences. Figure 5 shows typical surface roughness properties of the stone-ground ski base as obtained by scanning electron microscopy (SEM) and optical profilometry respectively:

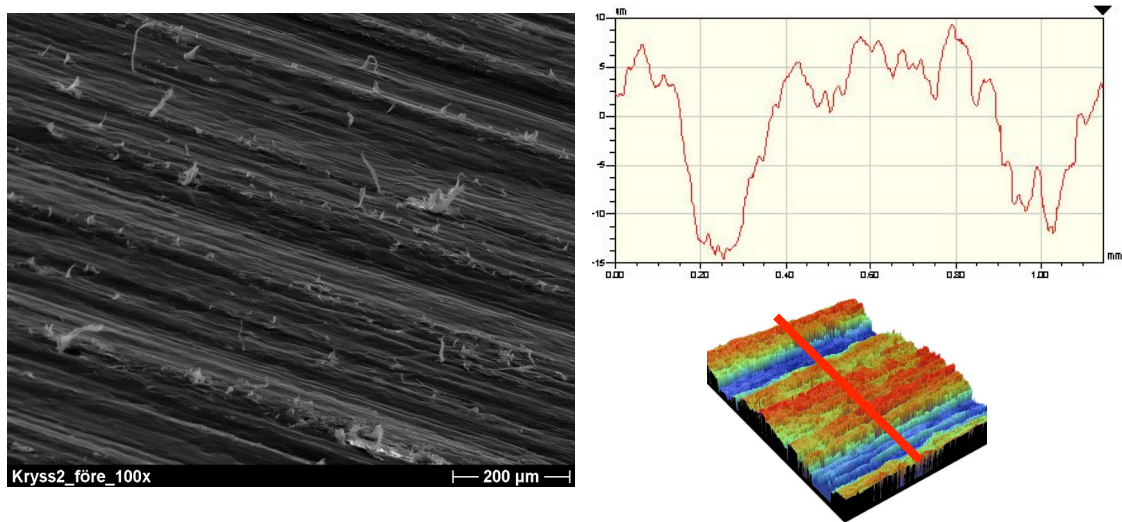


Figure 6: Typical stone-ground surface properties at 100x magnification. $R_A = 5.7\mu\text{m}$ and $R_T = 25\mu\text{m}$.

A stone-ground surface is very rough with an uneven and seemingly uncontrolled structure and many loose ends creating a carpet of hair. If the lubricated water film is assumed to be at a maximum about $1\mu\text{m}$ thick, this roughness will add a large proportion of ploughing. If the surface is waxed the roughness is somewhat refined and polished, see Figure 6:

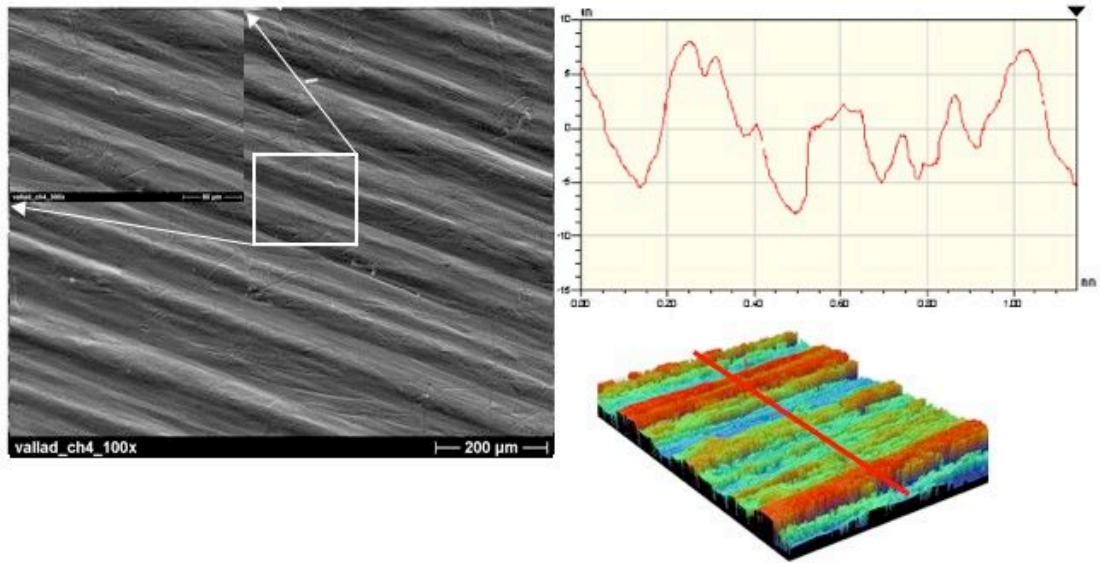


Figure 7: Typical CH₄-waxed surface of a ski base at 50x magnitude with $R_A = 3.37 \mu\text{m}$ and $R_T = 22 \mu\text{m}$.

For steel brushing, the hard metal brush will deform the surface in many spots causing a rugged carpet of sharp asperities, see figure 7:

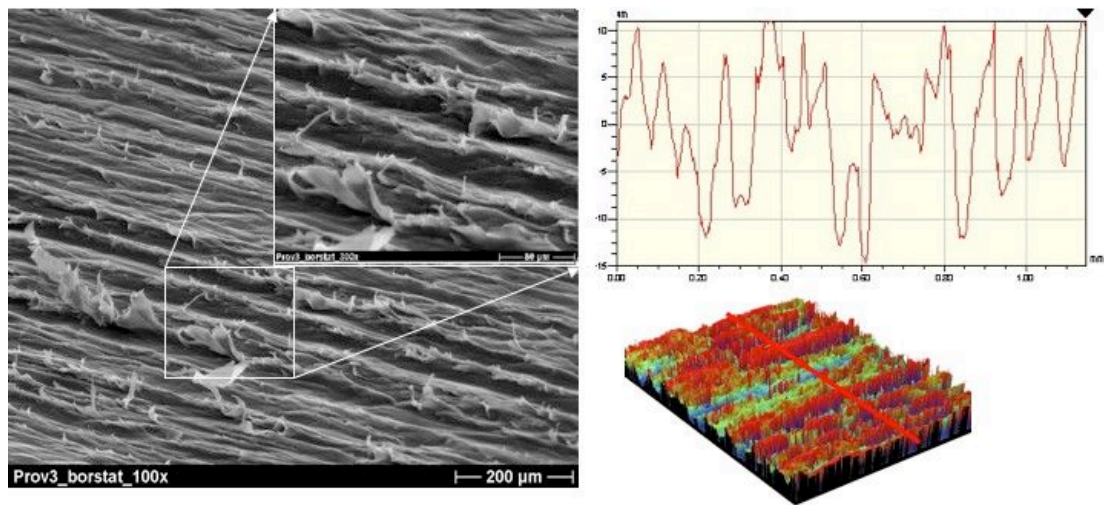


Figure 8: Typical steel brushed surface at 50x magnitude. $R_A = 5.4 \mu\text{m}$ and $R_T = 30 \mu\text{m}$.

If a softer polish brush is used, the surface will be similar to the waxed. This is expected since the final wax preparation step is soft brushing. See figure 8:

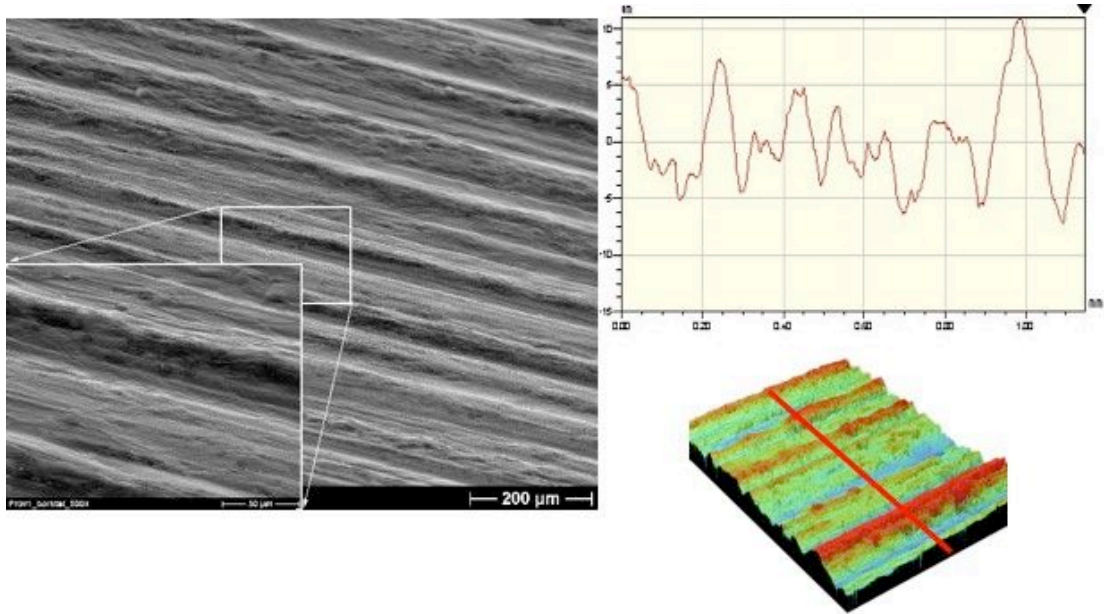


Figure 9: A nylon polish brushed surface with $R_A = 3.1 \mu\text{m}$ and $R_T = 23 \mu\text{m}$.

The surface is evidently improved in terms of roughness but still far to rough to not break through the lubricating water film. If a sharp cutting edge is used the result will get far closer to the assumed ideal, see figure 9:

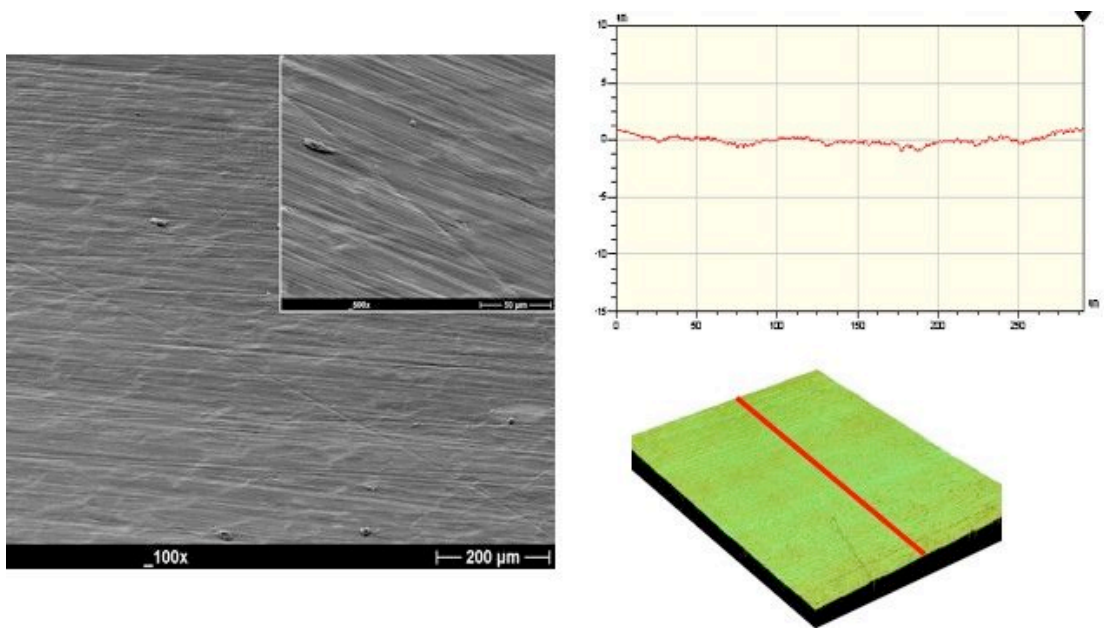


Figure 10: A cutting edge prepared ski base. The surface has a roughness of $R_A = 0.2 \mu\text{m}$ and $R_T = 1.2 \mu\text{m}$

When the surface is cut with a sharp edge a structure pattern is observed looking like a web upon the surface. This is believed to be the grain boundaries between the sintered grains. These boundaries have another elasticity allowing them to elastically yield under the edge and then to flex back, thus providing an unwanted structure.

It is also notable that the waxed and polish brushed all have very smooth ridges and measured alone they show typical R_A -values of 0.15-0.2 μm . On a hard and packed track, these surfaces will have a very low plough component compared to running on a soft and moisture track. Snow hardness and compaction will of course also affect the friction in that case.

3.2.4 Real contact area establishment

When a ski is pressed down upon the snow track, there will be a brief establishing of many contact spots during the compaction phase. Being a macroscopically soft material, snow will establish many real contact spots a_i . The size of these will still be determined by the hardness of solid ice of polyethylene depending on temperature. Still none of these spots are load carrying in a strict sense as the structure can be considered as collapsing during the compaction phase. When this is over the snow surface crystals can act as solid ice crystals and the contact area is down at tens of mm^2 as shown.

The density of snow and the inter-granular strength might also affect the ability to reorient the crystals along with the gliding direction, a behaviour indicated by B urle, [B au06].

3.3 Wear

Concluding that UHMWPE is the harder material, it might be expected that ice crystals together with snow matrix compaction will determine the contact area (4). It is harder to draw conclusions about wear mechanisms. Ducret et al shows that rough smaller surface edges are worn off while sliding on ice. The bulk of material and its structure are unaffected.

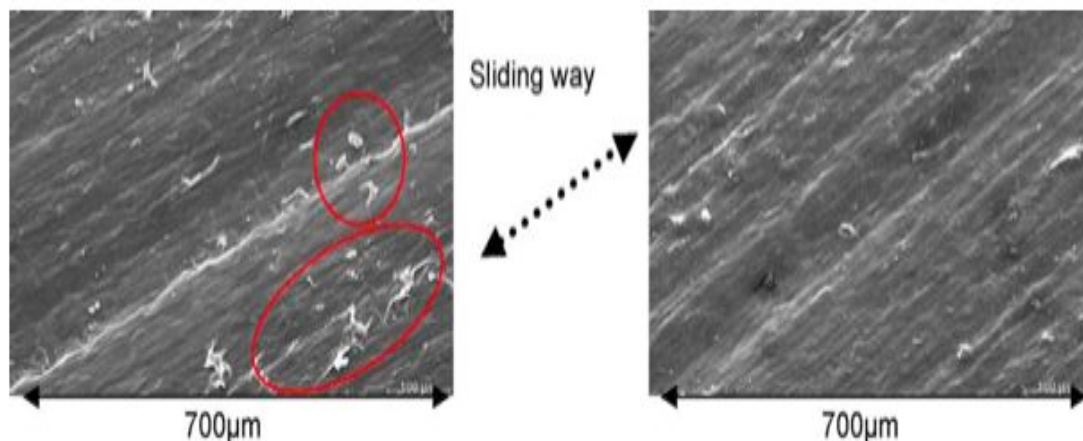


Figure 11: Typical wear of UHMWPE ski base. a: After stone-grinding b: After sliding against snow at -5°C and velocities $<0.1\text{ m/s}$. [Duc04]

At the university of Lule , Daniel Nilsson has with an in situ test shown that the ski base structure is worn during a number of long distance races [Nil07].

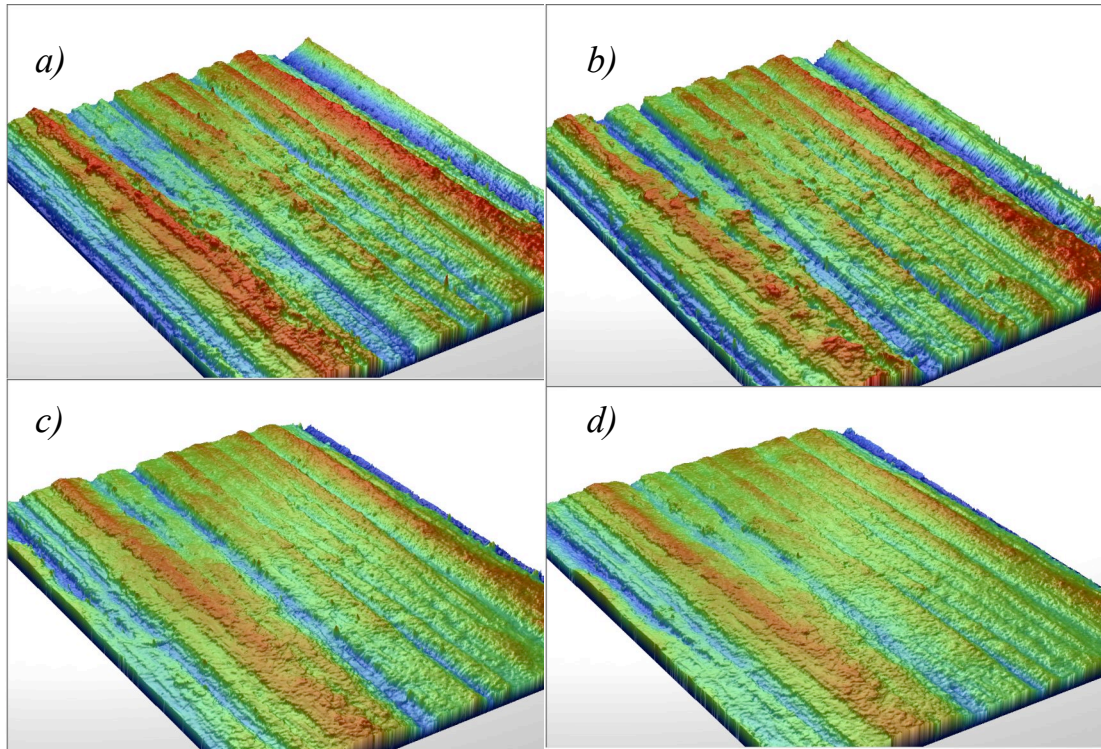


Figure 12: Ski base wear after a: Stone grinding, b: Wax preparation, c: Qualification race of Järnforan, 43 km, -13 °C, d: Vasaloppet 2007. The comparison is made on the exact same area. Note the major difference after the Järnforan race. [Nil07]

Assuming that elasticity properties of the materials correlate to microscopic hardness. Single crystalline ice can wear the ski base on the premises that the surface crystals are strongly enough bounded into the surface of the ski track. In this case it is no difference between snow and ice. If the matrix is not strong enough, the ski base surface peaks will rather reorient the surface ice crystals. The ski base has the potential to wear polycrystalline ice crystals at any time except when these are reoriented.

4. Experimental apparatus

4.1 Construction of custom made tribometer

The test rig is a custom made pin-on-disc/tribometer for use of ski base samples on snow and ice. The features follow classical mechanical principles and are discussed and presented here.

4.1.1 Basic

The body consists of a stainless steel-frame with two mounting levels. On the lower a steel plate is mounted with a fitting for a roller bearing. This is aligned with a fitting on the upper level mounted on a large cover plate. A motor attachment is mounted at the end of the frame where there is free space from the upper cover plate. The rotating disc is of a 500 mm diameter and can be rotated in both directions, although clockwise is chosen as the default direction.

All dimensions are adjusted to fit into a fridge given to the project by GB Glace AB.

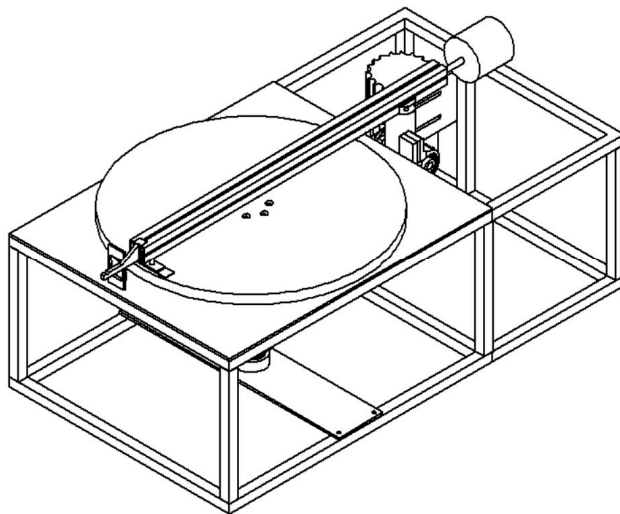
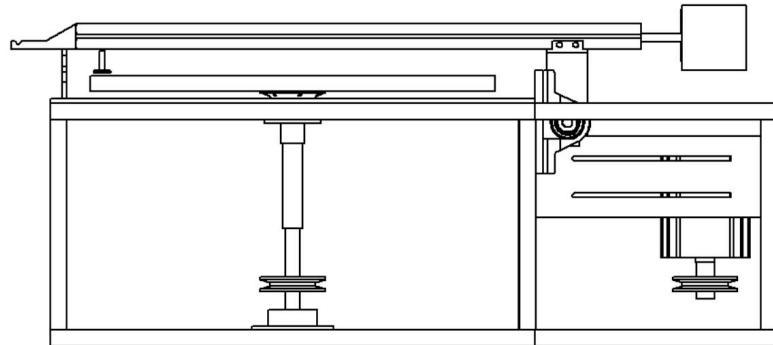


Figure 13: A panoramic view on the tribometer. The reminders from a vinyl player are not far away. The construction has an advantage in its mobility, it can be moved anywhere and be used outside next to a ski track.

4.1.2 Experimental setup

Side view



Top view

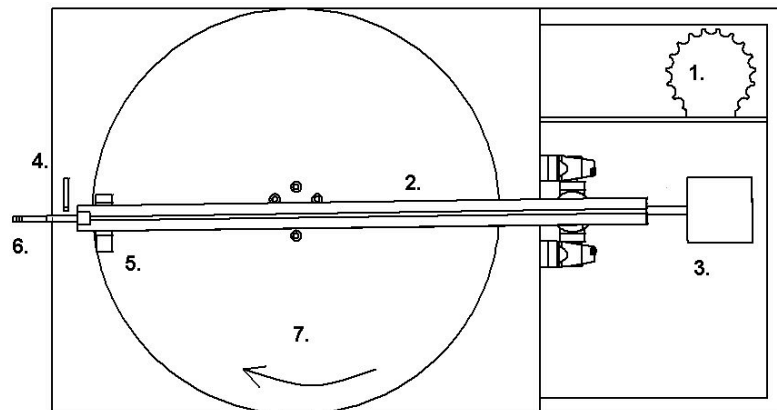


Figure 14: The main features of the tribometer. 1: Motor 2: Profile test arm. 3: Balance weight 4: Strain gauge bridge sensor 5: Ski sample 6: Normal load pin 7: Rotating disc.

4.1.3 Motor system

A 1,5kW 3-phase electric motor is vertically mounted onto the frame. An Omron frequency controller, not mounted onto the frame, controls the motor. The motor rod is pointed downwards in order to keep the dimensions within those of the frame. Also the heat from the motor will be passed straight upwards and can also be covered if necessary. The steel plates have a vertical rod running through the frame within the roller bearings. A disc is attached on top of the rod for the carrying on snow and ice, thus simulating a running ski track.

For preparation of the ski track, an arm with a cutting edge is applied onto the upper cover plate that prepares the disc surface with an even level.

4.1.4 Analytical equipment

The very ski base sample is mounted on a thin aluminium plate. This plate is of various sizes and contains a centred conical cavity as well as different geometrical openings for optical analysis.

An aluminium profile stretches over the rotating disc with a tip that can be loaded with external weights and a vertical pin that puts the load onto the conical cavity on the sample plate. The profile is balanced by a weight at the rear end. In order to have the lowest possible friction the profile is connected via two dry roller bearing that would allow the end of the profile, along with tip and sample, to move in the discs rotation direction. However a strain and pressure gauge holds the profile in constant place thus balancing all force given in the rotation direction i.e. the friction force. The gauge consists of two thin bearers with two strain gauges applied on each of them, creating a Wheatstone bridge. While using a strain gauge bridge-sensor and LabView-equipment, the obtained measurement resolution is 10^{-2} N.

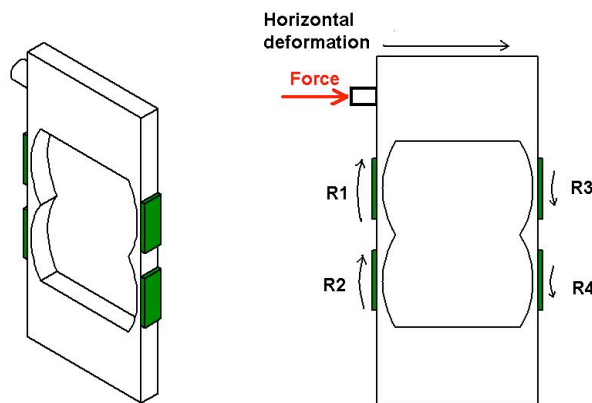


Figure 15: The strain gauge bridge-sensor. The force from the profile deforms the bearers while moving the top horizontally, causing the left gauges to extend and the right to shorten, causing the bridge to unbalance. A voltage indicating the magnitude of the force can be measured from the bridge.

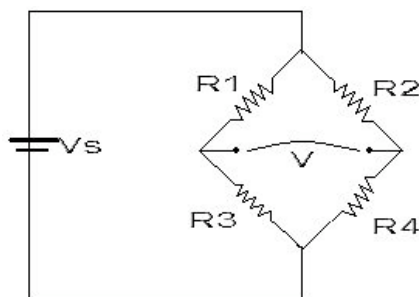


Figure 16: A schematic view over the Wheatstone bridge. The voltage V is zero when the four resistors are balanced i.e. when $R3/R1=R4/R2$.

The deformation of the resistors during load causes change in resistance due to extension/shortening of the resistor length and increase/decrease of the resistor section area. The voltage V is described below:

$$V = \left(\frac{R_4}{R_3 + R_4} - \frac{R_2}{R_1 + R_2} \right) V_s \quad (21)$$

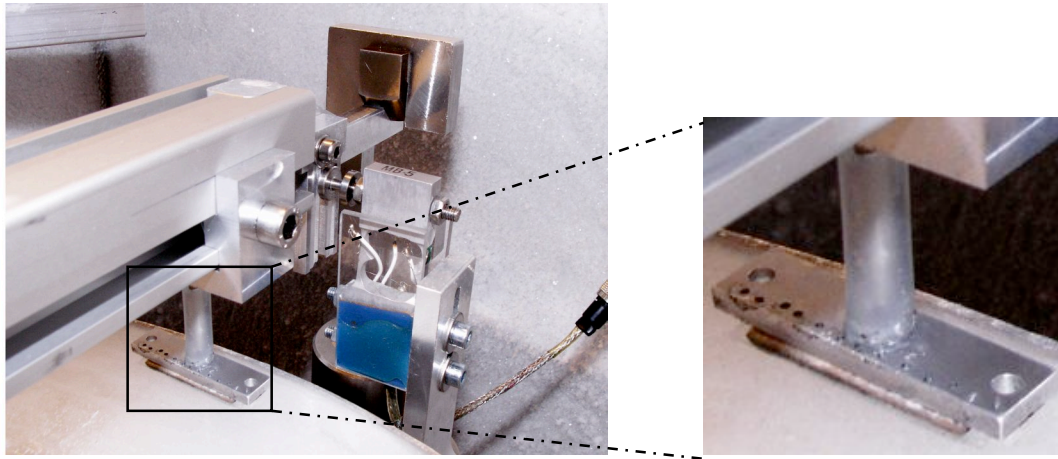


Figure 17: The profile rests on the pin placing the load on the sample holder at the left. The load is placed at the tip of the profile and the whole system is forced against the strain gauge-sensor to the right.

The profile is resting on two horizontal bearings allowing the user to lift the profile when operating or maintaining the rig.

The sample is mounted on a thin aluminium sample holder with a conical cavity. A pin from the aluminium profile is placed upon the sample and fitted into the cavity and thus placing the load. To avoid rotation of the sample due to the small perpendicular friction contribution from the disc, a rubber socket fitted onto the pin and glued onto the aluminium sample holder. This keeps the sample stable and still able to compensate rotation as well as rotation phenomena.

The aluminium plates also allow optical analysis with ultra violet and infrared light. Cameras for these purposes can be attached on an arm mounted at one of the corners of the rig.

A summary of the capacity and performance of the system is listed in table 1:

Table 1: Variable parameters in the experimental setup

System parameters	Value
Velocity	0.1-12 m/s
Load	0.5-15N
Air temperature	+20- -20°C
Force measurement resolution	10^{-2} N

4.2 Experimental

The test series for verification and validation of the test rig in general as well as the ability to evaluate different surface preparations are essential for the project. Due to practical reasons, only solid ice with a small roughness is slid upon. The parameters examined are summoned below:

- Velocity
- Load
- Temperature
- External water presence
- Surface roughness

Dry friction has no velocity dependence according to eq (5) and eq (9), therefore a relative constant friction coefficient should be found if dry conditions are dominating. If wet friction dominates then velocity dependence towards a linear proportion should be found according to eq (14).

Eq (5) and eq (6) shows that the friction coefficient is non-dependent on normal force, thus showing a proportional increase in contact area and therefore an equally proportional increase in friction force. For dry conditions and adhesive friction the friction coefficient should be constant.

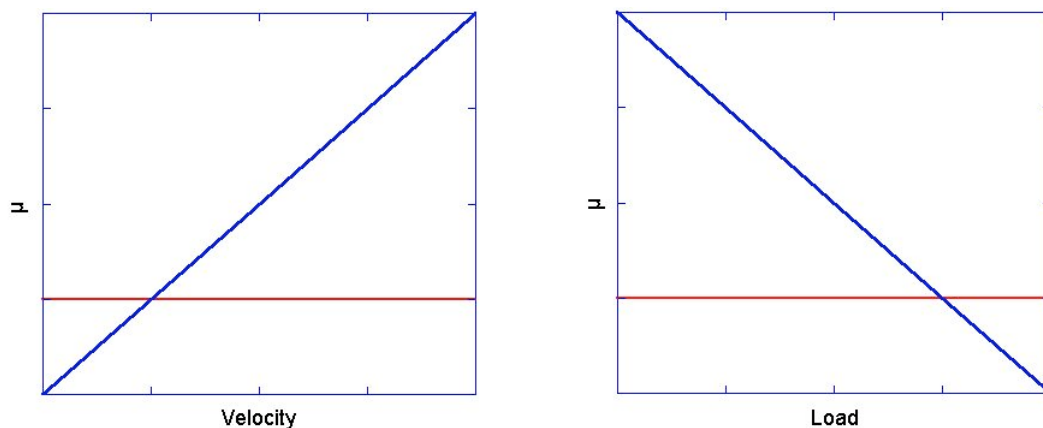


Figure 18: Ideal relations between friction coefficient, velocity and load respectively as predicted from theory. The red and blue slopes represent dry and wet friction respectively.

Since the changes of friction regimes are assumed to be dependent on friction heating, the temperature should have an impact on friction that could be described by the theory of both dry and wet friction.

The influence of water presence should be notable during any arbitrary condition. Thus adding water and/or heat to a stable system could give valuable indications of influences of friction.

The ploughing of the surface asperities is expected to influence during load variations where the friction coefficient consists of contributions from both adhesion and ploughing.

4.2.1 Test samples

For all general experiments, a stone-ground ski base surface from Fischer is used as a reference. The sample has a roughness of $R_a=5\ \mu\text{m}$ and $R_T=21\ \mu\text{m}$. For comparison between extremes, a smooth and a very rough surface are used.

The smooth sample has a roughness of $R_a=0.2\ \mu\text{m}$ and $R_T=2\ \mu\text{m}$, it is prepared with a Primateria scraper. The rough sample is brushed with a steel brush and has a $R_a=6\ \mu\text{m}$ and a $R_T=26\ \mu\text{m}$.

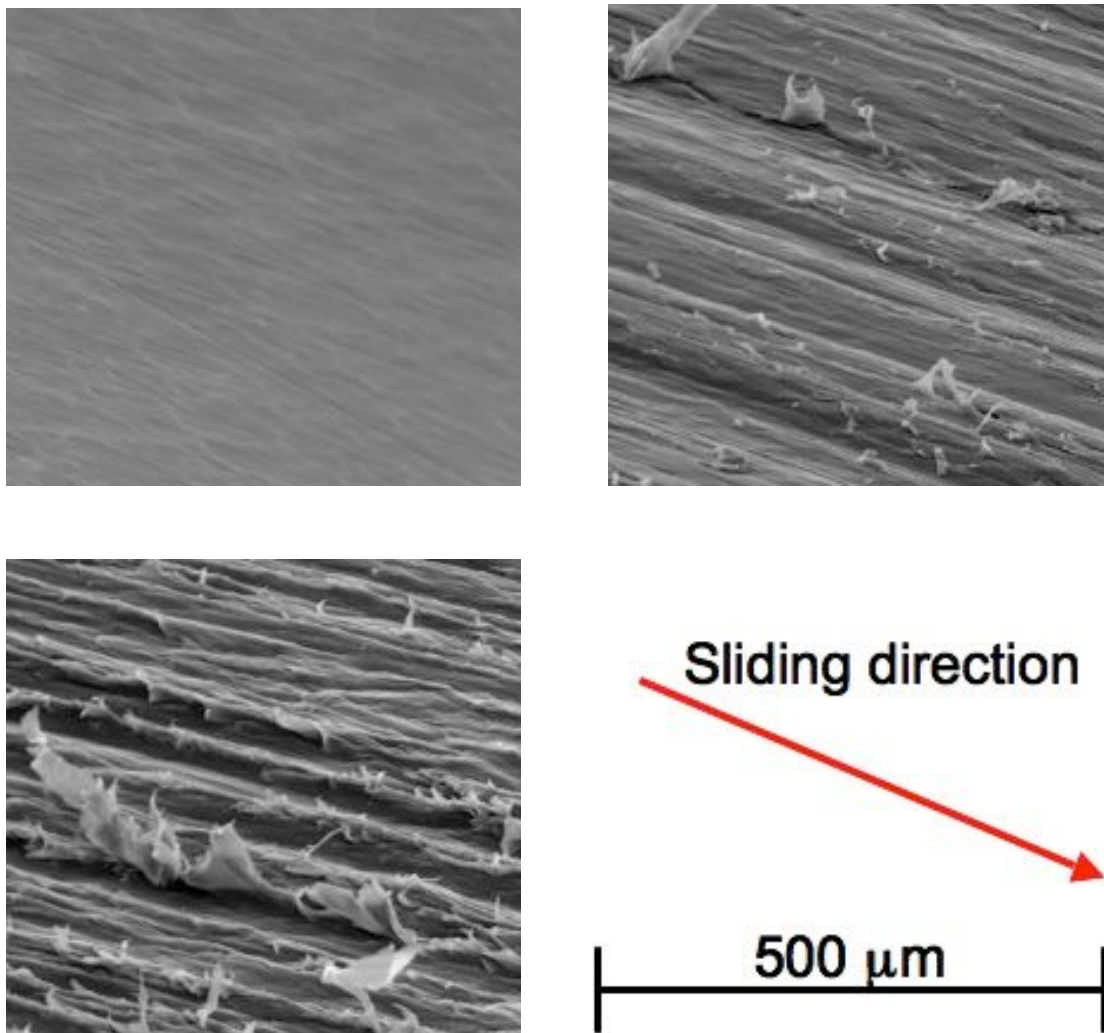


Figure 19: A comparison of the surfaces. The stone-ground surface in the middle with the smooth to the left and the rough to the right.

The apparent contact area is $4\ \text{cm}^2$ for all samples. External parameters are varied according to *Table 1*.

The experiment series for this thesis is of a surveying nature aiming for general behaviours and their variations rather than finding an absolute number for any parameter. The performed experiments can be seen in *Table 2*:

Table 2: The values are chosen to be typical for an 80kg person skiing at a moderate pace.

Ski base surface	<i>Stone-ground</i>	<i>Smooth</i>	<i>Rough</i>
Velocity dependence	v = 0.5-11 m/s F _N = 13.54N T = -14°C		
Load dependence	F _N = 0.5-20N v = 3.6 m/s T = -14°C, -5°C	F _N = 0.5-15N v = 3.6 m/s T = -14°C, -5°C	F _N = 0.5-15N v = 3.6 m/s T = -14°C, -5°C
Temperature dependence	T = -16°C - +/-0°C, v=3.6 m/s, F _N = 13.54N		

4.2.2 Track preparation

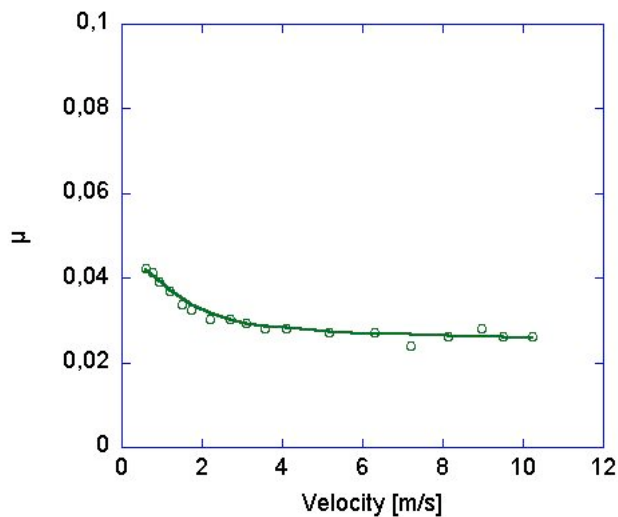
In order to achieve a running track with as small disturbances as possible, a lath tool is used to cut out a rail for the ski sample to run upon. The torque influence of a force component, perpendicular to the sample direction, caused by the rotation affecting as long as the sample is kept stable in its direction.

5. Results

5.1 Test apparatus

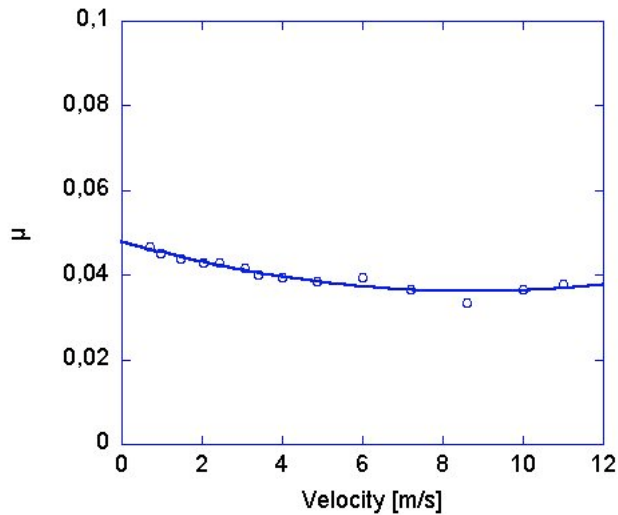
The function of the strain gauge bridge sensor is plausible and the system has a sufficient sensitivity. No variation of friction over time was observed for fixed conditions, thus it can be ruled out that the system with a rotating disc accumulates heat and therefore implicates time dependence. This is however not presented in details here.

5.2 Velocity dependence



Plot 1: Friction coefficient vs. velocity at -14°C at 12.93N load for a stone-ground surface.

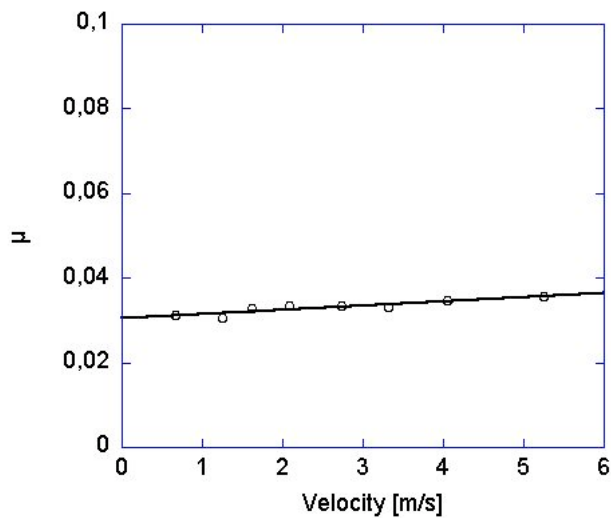
The friction is decreasing with two linear sections, at the beginning and the end respectively. For velocities up to 4 m/s there is a considerable drop in friction coefficient from about 0.043 to 0.028. At velocities between 4 and 10 m/s the velocity dependence is very low with the friction coefficient varying between 0.028 and 0.025.



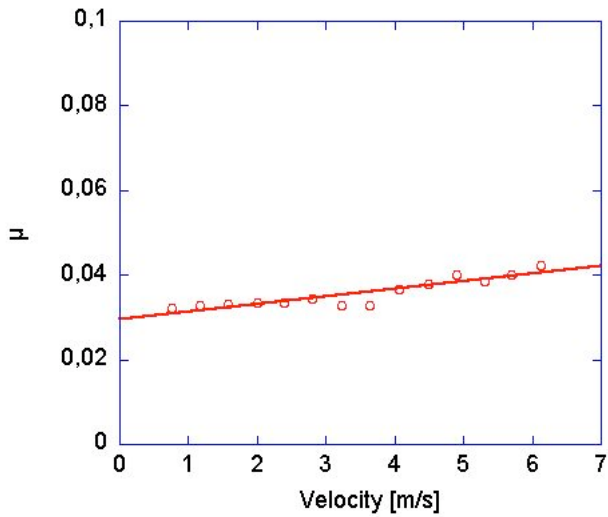
Plot 2: Friction coefficient vs. velocity at -5°C at 12.93N load for a smooth surface.

At -5°C the dependence is similar but a clear trend is observed. The initial drop is considerably lesser whilst a positive dependence can be imagined towards high velocities.

When temperature reaches close to the melting point. The velocity dependence is almost un-notable. A small linear increase for increased velocity is observed and this trend grows stronger if temperature is further increased.

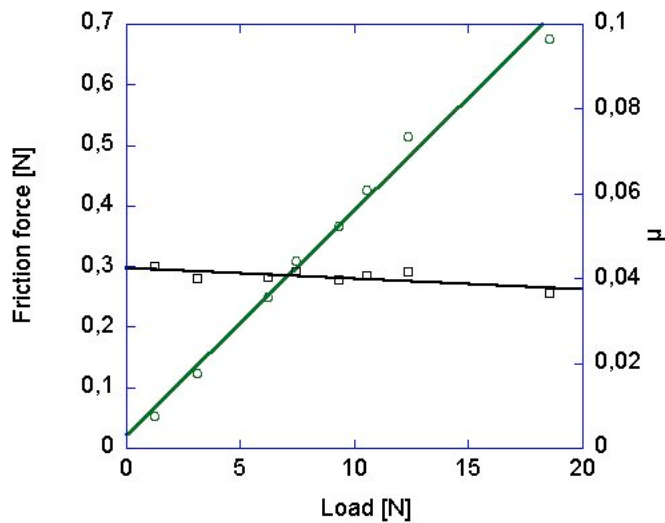


Plot 3: Friction coefficient vs. velocity at -1°C at 12.93N load for a smooth surface.



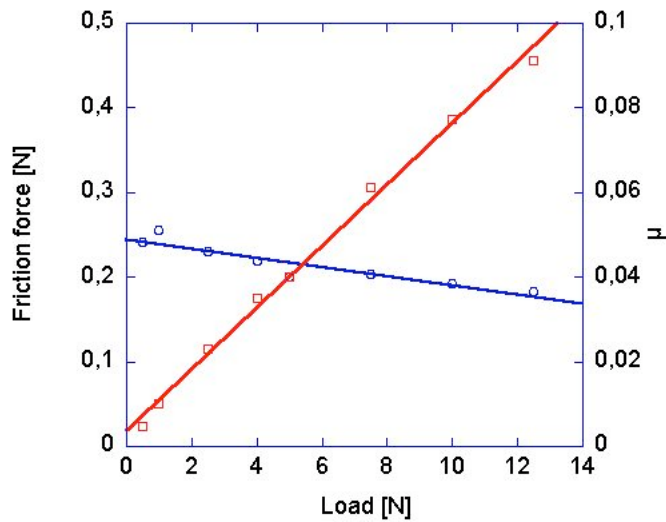
Plot 4: Friction coefficient vs. velocity at +1°C at 12.93N load for a smooth surface.

5.3 Load dependence



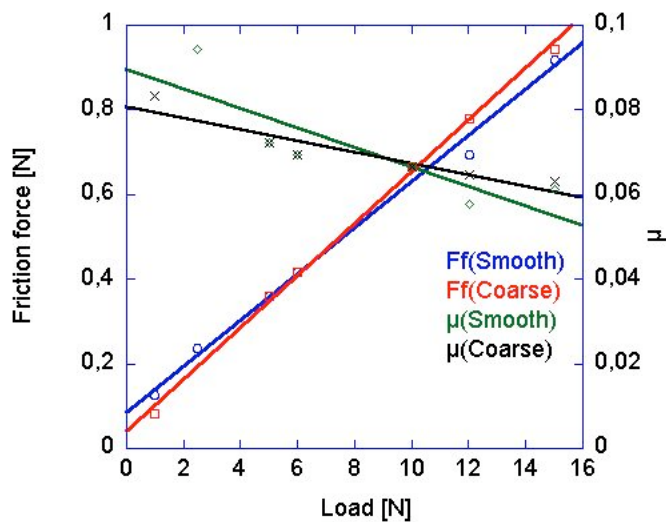
Plot 5: Friction force and coefficient vs. load at -14°C and 3.6 m/s velocity for a stone-ground surface.

At -14°C, the friction coefficient is rather constant with a small negative slope. The friction force is thus load proportional, although not entirely. Towards higher temperatures the friction coefficient has a more clearly negative slope. At higher temperatures, -5°C, the friction coefficient has a steeper slope.



Plot 6: Friction force and coefficient vs. load at -5°C and 3.6 m/s velocity for a stone-ground surface.

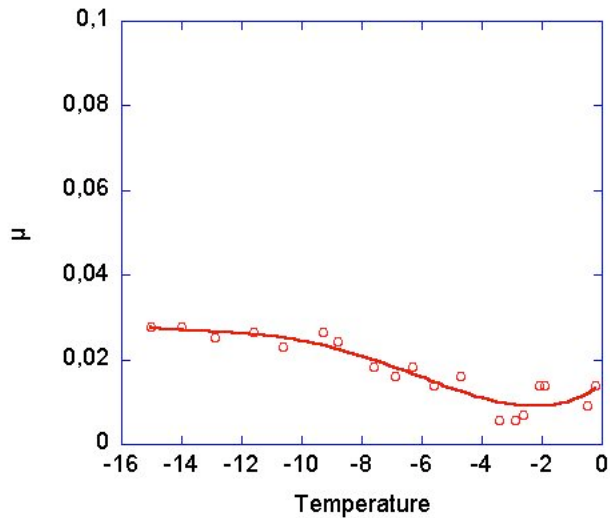
5.3.1 Surface comparison



Plot 5.2.5: Comparison between coarse and smooth sample on friction vs. load at -10°C and 12.93N load.

In a comparison between the smooth and the coarse surface no major differences could be seen when sliding on solid ice. The slope of the smooth curve fit is still somewhat lower than for the coarse as seen in figure 5.2.5. The friction coefficients are very similar with an almost un-notable difference but a small convergence towards higher loads. See figure 5.2.6:

5.4 Temperature dependence



Plot 5.3.1: Friction coefficient vs. temperature at 3.6 m/s and 12.93N load for a stone-ground ski base

The temperature dependence is observed as in figure 5.3.1. There is linearity from low temperatures up to -10°C where the friction varies from 0.028 to 0.025 and decreases into a new linear section with an inflexion point at about -6°C . The friction reaches its minimum 0.015 at about -2°C and then rises towards 0°C reaching the same friction as in the inflexion point.

6. Discussion

Friction as a measured magnitude is not a material parameter but rather a parameter connected to a certain system. Results are therefore more interesting concerning the trend variation against a parameter than the absolute numbers. The orders of magnitude for the friction coefficient of this ski base-ice system are expected and can be considered as correct. A smooth ice surface is assumed to decrease the characteristics of friction behaviour, nonetheless, clear results and their differences during varied conditions are found.

Predictions about important parameters were made out of a literature study concerning previous results and also out of general tribological theory. This method is well working for explanations and calculations of the friction coefficient. Most important are the actual deformation mechanisms. These are interpreted to be present in the results. There is however a need for further discussion of the validity of microscopic hardness the primary parameter for determining the real contact area. Hardness might not be a material parameter but rather a system parameter dependent of yield strength, fracture toughness and elasticity. The complex wear situation shown in section 3.3 strongly supports this. A closer focus should be put upon hardness and wear properties both within ice and UHMWPE. If the influence of these could be estimated and measured, improvements of both theory and practical applications would be achieved.

6.1 Test apparatus

There are practical issues regarding the correlation between laboratory results and the result for any skier. The general assumption that humidity follows air temperature is somewhat vague and only corresponds with snow humidity, according to Moldestads measurements. Also the variability of snow makes it difficult to recreate all possible conditions regarding water presence, density and snow-grain geometry. Since only one crystal phase exists in nature and all grain geometries seem to converge towards a spherical shape during melting and recrystallization, ice surfaces can be seen as an extreme and sometimes ideal case.

Difficulties in preparing a good snow track made it difficult to make topographical comparisons. This is however a problem that would be easier to overcome with a larger test environment than the present chest freezer. A problem in this freezer is the temperature control, which demanded a large amount of time.

6.2 Velocity dependence

The general friction decreased is believed to be due to the growth of the soft amorphous surface layer. This is reasonable since the heating trend would be less notable at higher temperatures where the friction is lower thus producing less heat, all in agreement with theory. The almost constant friction coefficient close to 0°C is

difficult to explain, it is perhaps due to growth compensation of area versus water film thickness at the lubricated contact spots. These behaviours are general for variations of load and time and still correspond well with the results of Lehtovaara and Baurle.

There are no clear limits between the different lubrication regimes. Dry conditions at low temperatures, boundary lubrication-like, still show vaguely, decreasing friction coefficients against both load and velocity. Whether this is caused by water or dry-like surface lubrication is not really relevant. At higher temperatures a mixed lubrication regime is observed, not even at temperatures above the melting point can fully lubricated behaviour be seen. Influence of water shearing is of course seen in the decreasing load and increasing velocity dependence against increasing temperature.

6.3 Load dependence

Strong linear dependence for friction force on load while the coefficient that remains rather constant, implicates adhesive friction in correspondence to theory. Due to topographic disturbance, the linearity is expected to be higher than for the ideal case. The minor slope of the friction coefficient is considered to be caused by mechanical wear of small rough asperities of the ice surface and perhaps some warming of the ski base.

The topography of the ski base shows no impact while sliding on ice. This is not expected on smooth ice since it determines the contact area and does not impose any large ploughing component. Whatever topography is on the ski base will not affect since the contact only occurs on the very top of the structure. However, for a ski surface, very rough compared to the ice track, topography can be expected to show differences in the load dependence when the plough component will be more present.

6.4 Temperature dependence

The initial linear behaviour at low temperature is due to the growth of the amorphous layer, correlating with the velocity dependence measurement. The decrease at higher temperatures, the amorphous layer grows according to the description of [Gol78] as well as friction heat and humidity provides an increased water presence. This enhances the state of mixed lubrication where dry and viscous friction shares the load and provides a small sum of friction contributions. The lubricating water film between the contact spots continues to grow until it reaches a critical point. This occurs at the friction minimum where a small contact area is sustained along with a maximum thickness of the water film.

When the squeeze out-effect is too large a large contact area is established on the cost of a low film thickness, causing an increase of friction. The mixed regime is now dominated by the viscous friction component and further presence of water might lead to a contact area of the entire ski and very high friction. The results show a form of Stribeck-curve corresponding well with Baurle's and Slotfeldt-Ellingsen's measurements. [Bäu06], [SIE-T83]

It has been suggested that the friction increase towards $\pm 0^{\circ}\text{C}$ depends on the softening of ice that provides an increasing contact area and thus increasing friction indicating a dry friction condition [SIE-T83]. This is found slightly incorrect when the shear stress of the ice decreases proportionally with hardness.

6.5 Surface preparation

At low temperatures and dry conditions, theory implicates a perfect longitudinally smooth ski base. Structure is proven to have little or no impact on friction when sliding against ice, but against a snow matrix it is expected to be an essential parameter. The ploughing mechanism is strongly contributing to the glide resistance.

For the mixed lubrication interval between -12°C and -2°C , the surface should still be smooth longitudinally to avoid ploughing. Any water film should still be able to grow in thickness during shearing thus causing less resistance. This should also be structurized in the perpendicular direction. This is due to the softer snow matrix and the increasing presence of water between the surfaces. The structure is suggested to be fine with a thin linear pattern. It could be necessary to break the pattern with another pattern in order to avoid unnecessary long contact with a single snow grain, causing too much melting. Still it must be coarse enough to avoid a large true contact area against squeezed out water. This might be present due to the small area of the contact spots, causing high pressure due to Lehtovaara's friction model.

At even higher temperatures exceeding -0°C , softness and elasticity modulus of the snow matrix and even the low ice crystal temperature is causing an increased contact area and contact spots. A vast amount of water present is a cause of further increasing contact area during snow compression where water can be squeezed out like from sponge. A deep structure suitable to break the contact area of non-load carrying water and to avoid ploughing would follow the earlier mentioned system of smoothness combined with a coarse structure.

The ideal structure concerning earlier mentioned properties is a subject for future research. The difficulty of calculating this implicates carefully undertaken experiments with high resolution. The test rig is a good tool for isolating parameters in order to resolute differences in topographical preparations.

7. Conclusions

7.1 Tribometer

- The test rig has a good sensitivity with a resolution of the friction coefficient of 0.01
- Observed measurements can be sufficiently described by the theoretical model.
- Measurements provided results in good agreement with theoretical predictions as well as previous literature.
- The experiments showed a plausible reproducibility.
- A better controlled temperature environment would result in more accurate temperature limits for the lubrication regimes.

7.2 Friction behaviour

- At temperatures below -12°C , no water lubrication is evident and the friction conditions can be described as dry. Increased load and velocity lowers the friction coefficient due to increased heat production in the surface interface.
- At temperatures between -10°C and -2°C , a mixed lubrication regime is dominating. Load dependence is decreasing and velocity dependence shows a minor friction coefficient increase versus increased velocity. The friction coefficient decreases against higher temperature reaching its minimum at -2°C .
- At temperatures near 0°C , viscous shear increases the influence on the friction. Velocity dependence is low and increases vs. further increased temperature. The friction coefficient increases generally due to increased contact area A_r .

7.3 Surface preparations

Preparations of surface topography corresponding to the friction behaviour:

- At dry friction conditions, a perfectly longitudinally smooth ski base with a minor topographic structure perpendicular to the gliding direction is suggested.
- Within the mixed regime, a deeper topography should be added. Still a smooth longitudinal topography is needed. In the perpendicular direction, the longitudinal pattern can be cut off or broken.
- For very wet conditions, the topography should be very deep to avoid contact area increase for non-load carrying water.
- Valleys and ridges of the structure should always be smooth in the motion direction.

References

- [Amb81] W. Amback, B.Mayr, *Ski gliding and water film*, Cold Regions Science and Technology, 5 (1981), p.59-65
- [Bow53] F.P. Bowden, *Friction on snow and ice*, Cambridge University Press Series A, Cambridge, 217 (1953), p. 462-478
- [But58] T.R Butkovich, *Hardness of single ice crystals*, The American Mineralogist, 43 (1958), p.48-57.
- [Bäu06] L. Bäurle, *Sliding Friction of Polyethylene on Snow and ice*, Dissertation submitted to the Swiss Federal Institute of Technology Zurich, nr 16517 2006.
- [Col95] Petrenko Victor F, Colbeck Samuel C, *Generation of electric fields by ice and snow friction*, Journal of Applied Physics, 77:9 (1995), p. 4518-4521
- [Dan04] X.Dangsheng, *Friction and wear properties of UHMWPE composites reinforced with carbon fibre*, Materials Letters, 59 (2005), p. 175-179
- [Duc04] S.Ducret, H.Zahouani, A.Midol, P.Lanteri, T.G. Mathia, *Friction and abrasive wear of UHMWPE sliding on ice*, Wear, 258 (2005), p. 26-31
- [Epi03] V.P. Epifanov, *Rupture and Dynamic hardness of Ice*, Doklady Physics, 49 (2004), p. 86-89
- [Gol78] I.Golecki, C. Jaccard, *Intrinsic surface disorder in ice near the melting point*, Journal of Physics C: Solid State Physics, 13 (1978), p. 4229-4237
- [Gow74] A.J. Gow, *Time-temperature dependence of sintering in perennial isothermal snowpacks*, Proceedings of the Grindelwald symposium, 114 (1974), p. 25-41
- [Hen89] P.J. Henderson, A.J. Wallace, *Hardness and creep of cross-linked polyethylene*, Polymer, 30 (1989), p. 2209-2214
- [Jac05] S. Jacobson, S. Hogmark, *Tribologi*, Andra upplagan, Uppsala Universitet, Uppsala 2005
- [Kat74] T.Katutosi, *The temperature dependence of hardness of snow*, Proceedings of the Grindelwald symposium, 114 (1974), p.103-109
- [Leh89] A. Lehtovaara, *Kinetic friction between ski and snow*, Dissertation at the University of Helsinki, 1989

- [Lib05] K.G. Libbrecht, *The physics of snow crystals*, Reports on Progress in Physics, 68 (2005), p.855-895
- [Liu99] C.Liu, L.Ren, R.D. Arnell, J. Tong, *Abrasive wear behaviour of particle reinforced ultrahigh molecular weight polyethylene composites*, Wear, 225-229 (1999), p. 199-204
- [Lon06] J. Long, P. Chen, *On the role of energy barriers on determining contact angles*, Advances in Colloid and Interface Science, 127 (2006), p. 55-66
- [Mo199] Moldestad, D.A. (1999): *Some Aspects of Ski Base Sliding Friction and Ski Base Structure*. Dissertation, 1137 (1999), Norwegian University of Science and Technology
- [Nil07] D. Nilsson, *Ytkarakterisering av skidbelag i olika stadier av inkörning*, Luleå Universitet 2007
- [Pav07] V.P Pavlenko, L. Rosenqvist, *Fluid mechanics*, second edition, Uppsala University, Uppsala 2007
- [Pet03] J.J. Petrovic, *Review Mechanical properties of ice and snow*, Journal of Materials Science, 38 (2003), p. 1-6
- [Pit98] B. Pittenger, D.J. Cook, C.R. Slaughterbeck, S.C. Fain Jr, *Investigation of ice-solid interfaces by force microscopy: Plastic flow and adhesive forces*, Journal of Vacuum Science Technology A, 16:3 (1998), p. 1832-1837
- [Rav02] U. Raviv, S. Giasson, J. Frey, J.Klein, *Viscosity of ultra-thin water films confined between hydrophobic or hydrophilic surfaces*, Journal of Physics: Condensed Matter, 14 (2002), p. 9275-9283
- [SIE-T83] D. Slotfeldt-Ellingsen, L. Torgersen, *Water in ice: Influence on friction*, Journal of Physics D: Applied Physics, 16 (1983), p. 1715-1719.
- [Sko53] J. Skotnický, *The dependence of the melting point on the pressure*, Czechoslovakian Journal of Physics, 3 (1953), p. 225-230
- [Spr84] E. Spring, *Mätning av friktionskoefficienten för skidor glidande på snö*, Presented at NORDTRIB August 15-17 1984
- [Str98] H.Strausky, J.R. Krenn, A. Leitner, F.R. Aussenegg, *Sliding plastics on ice: fluorescence spectroscopic studies on interface water layers in the μm thickness regime*, Applied Physics B: Lasers and Optics, 66 (1998), p.599-602
- [Suw98] K. Suwanprateb, *Time-dependent hardness of particulate-filled composites*, Journal of Materials Science, 33 (1998), p. 4917-4921

- [Tor03] L. Torris, C. Gentile, A.M. Visco, N. Campo, *Wetting modification on uhmwpe surfaces induced by ion implantation*, *Radiation Effects and Defects in Solids*, 158:10 (2003), p. 731-741
- [War84] S.G. Warren, *Optical constants of ice from the ultraviolet to the microwave*, *Applied Optics*, 23:8 (1984), p. 1206-1225
- [Wie06] K.A. Wier, T.J. McCarty, *Condensation on Ultrahydrophobic Surfaces and Its Effect on Droplet Mobility: Ultrahydrophobic Surfaces Are Not Always Water Repellant*, *Langmuir*, 22 (2006), p. 2433-2436
- [Öne00] D. Öner, T.J. McCarthy, *Ultrahydrophobic Surfaces. Effects of Topography Length Scales on Wettability*, *Langmuir*, 16 (2000), p. 7777-7782

Web sources

- [Gur08] Gurit AG, *Ski & Snowboard Running Bases*, manufacturing guide of ski bases.